HAYATI
Journal of Biosciences

Vol. 32 No. 6, November 2025 1626-1642
DOI:10.4308/hjb.32.6.1626-1642
ISSN: 1978-3019
EISSN: 2086-4094

Research Article

Comparative Study of DNA Barcoding and Mini-Barcoding based on COI Gene for Species Identification and Phylogeny of Formicidae Family (Insecta: Hymenoptera)

Beivy Jonathan Kolondam[1], Trina Ekawati Tallei[2*], Roni Koneri[2], Juliet Merry Eva Mamahit[1]

[1]*Doctoral Program of Entomology, Postgraduate Program, Sam Ratulangi University, Manado 95115, Indonesia*
[2]*Department of Biology, Faculty of Mathematics and Natural Sciences, Sam Ratulangi University, Manado 95115, Indonesia*

ARTICLE INFO

Article history:
Received May 17, 2025
Received in revised form July 12, 2025
Accepted August 11, 2025
Available Online September 1, 2025

KEYWORDS:
Ants,
DNA barcoding,
mini-barcoding,
phylogeny,
universal primer

ABSTRACT

DNA barcoding and mini-barcoding are widely used to study insect biodiversity, including ants (Hymenoptera: Formicidae). This study evaluated the effectiveness of both approaches for species identification and phylogenetic inference in ants, with particular attention to the performance of universal primers during PCR amplification. Full-length DNA barcode (658 bp) and mini-barcode (127 bp) regions of the mitochondrial cytochrome c oxidase subunit I (COI) gene were retrieved from GenBank, aligned, and analysed with maximum-likelihood phylogenetics (1,000 bootstrap replicates) under the Tamura-Nei model. The universal DNA barcoding primers (Folmer's LCO1490 and HCO2198) showed generally good alignment with ant COI sequences. However, multiple nucleotide mismatches were observed in LCO1490, including one critical mismatch located within the GC clamp region. In contrast, the universal mini-barcoding primers (UniMinibarF1 and UniMinibarR1) showed critical mismatches at their 3′ ends, likely reducing PCR efficiency. Despite limitations associated with primer mismatches, both DNA barcoding and mini-barcoding are reliable for species identification. DNA barcoding and mini barcoding are both capable of distinguishing ants at the species level, regardless of the length of the sequences being compared. The same sequences have also been used for phylogenetic analysis, showing good ability to distinguish ant species based on phylogenetic tree reconstruction. The comparison of DNA barcoding and mini-barcoding in ants showed that longer sequences offered superior resolution for species identification and phylogenetic reconstruction. These findings underscore the need for primer optimisation in ant-specific applications and highlight the utility of both barcoding strategies for taxonomic and evolutionary studies.

1. Introduction

DNA barcoding has emerged as a powerful genomic tool for species identification and biodiversity assessment, significantly accelerating the discovery and classification of taxa across diverse ecosystems (Gostel and Kress 2022; Antil *et al.* 2023). The standard DNA barcode for animals, a 658 base pair region of the mitochondrial cytochrome c oxidase subunit I (COI) gene, has demonstrated approximately 98 percent accuracy in resolving species boundaries in major taxonomic groups, including arthropods, birds, fish, and mammals (Hebert *et al.* 2003). By enabling sequence-based comparisons with curated reference libraries, DNA barcoding allows for accurate identification even when morphological characters are ambiguous or cryptic (Lombogia *et al.* 2020). This molecular approach has transformed several applied and theoretical fields, including biosecurity (Niemann *et al.* 2022), cryptic species detection (Wang *et al.* 2020), paleogenomics (Abdelhady *et al.* 2024), and forensic biology (Nithaniyal *et al.* 2021). Its global applicability is supported by initiatives such as the

* Corresponding Author
E-mail Address: trina_tallei@unsrat.ac.id

Barcode of Life Data Systems (BOLD), which provides access to large-scale sequence libraries and integrative taxonomic tools (Ratnasingham and Hebert 2007).

Recent advances have further expanded the utility of barcoding by integrating *in silico* workflows that simulate marker performance, assess primer universality, and predict amplification success before any wet-lab work is undertaken (Ficetola *et al.* 2010; Wang *et al.* 2023; Kalendar *et al.* 2024). However, despite these advances, no previous study has systematically compared the effectiveness of full-length DNA barcoding versus mini-barcoding regions in ants using *in silico* primer-binding analysis and phylogenetic assessment. In insects, comparative performances of DNA barcoding and mini-barcoding have been conducted on several orders (Virgilio *et al.* 2010). In the order Hymenoptera, this study has only been conducted on aphid bees (Gonçalves *et al.* 2022). The lack of comparative insight presents a methodological gap in barcode optimization for ant taxonomy, particularly when dealing with degraded DNA.

Although most DNA barcoding studies have relied on recently collected, well-preserved specimens with intact DNA, increasing attention has been given to the potential of using degraded materials (Hajibabaei *et al.* 2006; Ogiso-Tanaka *et al.* 2025). These include processed biological products, decayed tissues, and archival samples housed in museum collections (Mason *et al.* 2011; Nachman *et al.* 2023). The DNA in such materials is often fragmented as a result of exposure to varying preservation methods, such as pinning, desiccation, or treatment with chemicals like formaldehyde, all of which compromise molecular quality (Mason *et al.* 2011; Mitchell and Rawlences 2021). Nonetheless, these historical specimens are essential for taxonomic studies, particularly for rare, endangered, or extinct species. Their inclusion allows researchers to link genetic information with morphological traits from type material and to clarify taxonomic boundaries (Prosser *et al.* 2016; Yang *et al.* 2018). Advances in *in silico* primer design and mismatch analysis now allow researchers to predict amplification success from fragmented templates, thereby guiding experimental strategies for such challenging samples (Li *et al.* 2008; Francis *et al.* 2017; Wang *et al.* 2023; Huang *et al.* 2024). This study was therefore needed to inform primer selection for both high- and low-quality DNA templates in ants and to improve barcode-based species identification through computationally guided strategies.

To address the limitations of standard barcoding in degraded DNA, the mini barcoding approach has been developed. The mini-barcoding approach has been developed to overcome the limits of conventional DNA barcoding in degraded DNA templates. Mini barcodes are shorter regions within the COI gene, typically ranging from 100 to 300 base pairs in length (Meusnier *et al.* 2008). These shorter sequences retain sufficient taxonomic information to allow reliable species identification from degraded samples and, in some cases, offer resolution comparable to that of full-length barcodes in detecting intraspecific genetic variation (Xing *et al.* 2020; Liu *et al.* 2023). Because dozens of alternative mini-barcode primer pairs exist, *in silico* screening, which covers primer degeneracy, binding efficiency, and predicted taxonomic coverage, has become indispensable for selecting the most informative fragment for a given study system.

Ants (Formicidae) represent one of the most ecologically dominant and taxonomically diverse insect groups, with more than 13,000 described species and many more likely to be discovered (Messer *et al.* 2016; Cuautle *et al.* 2020). As key ecosystem engineers and bioindicators, ants contribute to nutrient cycling, soil aeration, seed dispersal, and population regulation of other invertebrates (Parr and Bishop 2022; Rocher *et al.* 2022). Their sensitivity to environmental change makes them valuable for ecological monitoring, particularly in response to habitat degradation, pollution, and climate change (Menta and Remelli 2020; Zhang *et al.* 2023). Ants serve as valuable bioindicators due to their sensitivity to environmental changes, making them useful for assessing the health of ecosystems. By monitoring changes in ant communities, it becomes possible to gain important insights into the broader ecological impacts of human activities like deforestation, urbanization, and agricultural expansion (Zina *et al.* 2021; Fotso Kuate *et al.* 2022; Wanna *et al.* 2022). Their importance in agriculture and pest management further underscores the value of preserving ant diversity.

The widespread availability of mitochondrial DNA (mtDNA) sequence data, particularly the COI gene, in public databases such as BOLD (https://boldsystems.org/) and GenBank (https://www.ncbi.nlm.nih.gov/nucleotide/) has enabled unprecedented insights into genetic diversity across ant (Formicidae) lineages (Kolondam *et al.* 2023). This wealth of data has revealed substantial barcode gaps, highlighting the effectiveness of COI for species identification within this ecologically

dominant insect group. These findings present a valuable opportunity for *in silico* comparative studies between full-length DNA barcoding and mini-barcoding approaches. By leveraging existing COI records, researchers can evaluate the taxonomic resolution and phylogenetic performance of shorter COI fragments, which are especially useful when working with degraded or low-quality DNA from museum specimens or environmental samples. *In silico* analysis also facilitates the refinement of universal and lineage-specific primers, improving PCR success rates across diverse ant taxa.

This study aimed to evaluate the diagnostic performance of full-length barcodes and multiple candidate mini-barcode regions in ants (Hymenoptera: Formicidae) through comprehensive *in silico* analyses. Specifically, publicly available COI sequences were mined, primer binding was simulated, and mismatch frequencies were quantified across taxa. Phylogenies were constructed to compare the resolution between full and mini fragments. These steps provided a benchmark for selecting primer sets suitable for highly degraded or low-quality ant DNA, while also highlighting the utility of computational pre-screening in streamlining downstream laboratory workflows.

2. Materials and Methods

2.1. COI Gene Sequence Collection

A total of 31 ant species (Hymenoptera: Formicidae) with publicly available mitochondrial COI gene sequences were selected from GenBank (https://www.ncbi.nlm.nih.gov). Species were chosen based on the credibility of the associated publications or the reputation of the submitting authors to ensure reliable taxonomic identification. The COI gene region was extracted by referencing gene annotations within the mitochondrial genome, where the full-length gene spans approximately 1,500 base pairs. Details of the selected specimens, including accession numbers and relevant references, are provided in Table 1.

2.2. *In Silico* Comparison of Primer Annealing Sites

All COI gene sequences of 31 ant species (Hymenoptera: Formicidae) were retrieved from GenBank and recorded in Geneious Prime (version 2025.0.3). The selected sequences were aligned using the MUSCLE algorithm (Edgar 2004). The two primer pairs were included in the analysis: the standard DNA barcoding primers LCO1490 and HCO2198 (Folmer *et al.* 1994), and the universal mini barcoding primers UniMinibarF1 and UniMinibarR1 (Meusnier *et al.* 2008).

The reverse primers were processed using the OligoAnalyzer tool (Owczarzy *et al.* 2008) to generate their reverse complement sequences, which were then aligned with the corresponding 3' binding sites of the COI sequences. Forward primers were directly aligned with the forward primer binding regions. Nucleotide mismatches between each primer and its corresponding binding site were examined at every position, with particular attention given to mismatches occurring at the 3′ end, which are known to affect PCR efficiency significantly.

2.3. Comparison of Species Identification Using DNA Barcoding Versus Mini Barcoding

Following the evaluation of primer binding sites, the effectiveness of both DNA barcoding and mini barcoding in differentiating ant species was assessed. This evaluation involved performing multiple sequence alignments in the same manner as described above, but with the primer binding regions excluded from the COI sequences to avoid bias in sequence similarity analysis. For DNA barcoding, the comparison focused on a 658-base pair fragment, commonly referred to as the "Folmer region". In contrast, mini barcoding targeted a shorter 127 base pair region corresponding to the expected amplicon of the universal mini barcode primers.

Multiple sequence alignment (MSA) was performed using the MUSCLE algorithm in Geneious Prime, and pairwise sequence comparisons were made both within species (intraspecific) and between species (interspecific) for each dataset. These comparisons were used to evaluate and compare the discriminatory power of DNA barcoding and mini barcoding for ant species identification.

2.4. Phylogenetic Reconstruction Using DNA Barcoding Versus Mini Barcoding

To examine the phylogenetic resolution provided by each COI fragment, separate phylogenetic trees were constructed using the full-length (658 bp) and mini barcode (127 bp) datasets. Sequence alignments for each dataset were performed using MUSCLE, and phylogenetic trees were generated using the Maximum Likelihood method implemented in PhyML version 3.3.20180621 (Guindon *et al.* 2010), which is integrated into Geneious Prime.

Table 1. Selected COI gene sequence of ants from GenBank for analysis

#	Specimen	Accession number	Reference
1	*Myrmica scabrinodis*	NC_026133.1	Babbucci *et al.* (2014)
2	*Pristomyrmex punctatus*	AB556947.1	Hasegawa *et al.* (2011)
3	*Linepithema humile*	MT890564.1	Park *et al.* (2021a)
4	*Linepithema humile*	NC_045057.1	Duan *et al.* (2016)
5	*Solenopsis geminata*	HQ215537.1	Gotzek *et al.* (2010)
6	*Dolichoderus sibiricus*	MK801110.1	Park *et al.* (2019c)
7	*Dolichoderus sibiricus*	MW160468.1	Park *et al.* (2019c)
8	*Dolichoderus quadripunctatus*	NC_049088.1	Park *et al.* (2020a)
9	*Dolichoderus sibiricus*	MH719017.1	Park *et al.* (2019c)
10	*Dolichoderus sibiricus*	NC_041075.1	Park *et al.* (2019c)
11	*Dolichoderus sibiricus*	MT919976.1	Park *et al.* (2020a)
12	*Formica selysi*	KP670862.1	Yang *et al.* (2016)
13	*Formica fusca*	NC_026132.1	Babbucci *et al.* (2014)
14	*Monomorium pharaonis*	NC_051486.1	Park *et al.* (2023)
15	*Leptomyrmex pallens*	NC_023093.1	Berman *et al.* (2014)
16	*Stenamma impar*	MT357021.1	Qian and Wu (2022c)
17	*Stenamma expolitum*	MT357020.1	Qian and Wu (2022b)
18	*Stenamma diecki*	MT357019.1	Qian and Wu (2022a)
19	*Brachyponera chinensis*	MT215089.1	Park *et al.* (2021b)
20	*Solenopsis invicta*	HQ215538.1	Gotzek *et al.* (2010)
21	*Stigmatomma silvestrii*	MT215092.1	Park *et al.* (2021c)
22	*Ooceraea biroi*	QOIP01000140.1	McKenzie and Kronauer (2018)
23	*Pachycondyla annamita*	OQ629337.1	Lin and Song (2023)
24	*Acropyga pallida*	NC_046425.1	Duan and Qian (2023)
25	*Ochetellus glaber*	MN044390.1	Park *et al.* (2020b)
26	*Ectomomyrmex javanus*	MK496222.1	Park *et al.* (2019b)
27	*Cryptopone sauteri*	MK138572.1	Park *et al.* (2019a)
28	*Tapinoma melanocephalum*	MN397938.1	Du *et al.* (2019)
29	*Acropyga goeldii*	MH158403.1	Duan and Qian (2020)
30	*Camponotus atrox*	KT159775.1	Kim *et al.* (2016)
31	*Monomorium triviale*	LC605004.1	Idogawa *et al.* (2021)

The Tamura-Nei model (Tamura and Nei 1993) was applied for both datasets, and node support was evaluated using 1,000 bootstrap replicates. The resulting phylogenies were then analyzed to assess clustering patterns and overall resolution, allowing direct comparison of the performance of full-length and mini barcode regions in reconstructing evolutionary relationships among ant species.

3. Results

3.1. *In Silico* Comparison of Primer Annealing Sites

The primer attachment sites were analysed to determine the length of the PCR amplicons. Multiple sequence alignment of the COI gene universal primer pair (Folmer *et al.* 1994) with 31 full-length COI gene sequences of ants revealed the primer attachment sites. The alignment began at nucleotide position 17, corresponding to the 5' end of the LCO1490 primer, as shown in Figure 1, and ended at nucleotide position 725, corresponding to the 5' end of the HC02198 primer, as shown in Figure 2. The HC02198 primer in Figure 2 was represented by its complementary sequence. These primer attachment sites produced a 709 bp amplicon in the PCR of ant samples, containing a 658 bp sequence known as the "Folmer region" (from nucleotide position 42 to 699), which was used for DNA barcoding.

Incorporation of the universal primer pair for mini-barcoding (Meusnier *et al.* 2008) into the sequence alignment revealed that the forward primer UniMinibarF1 overlapped with the DNA barcoding forward primer LCO1490 at nucleotide positions 19 to 41 (Figure 1). Both forward primers initiated at approximately the same upstream location, with UniMinibarF1 spanning nucleotide positions 19 to 44. On the downstream side, the reverse primer UniMinibarR1 was aligned at nucleotide positions 172 to 195 (Figure 3), resulting in a predicted PCR amplicon of 177 base pairs. This amplicon included a 127-base pair region, located between nucleotide

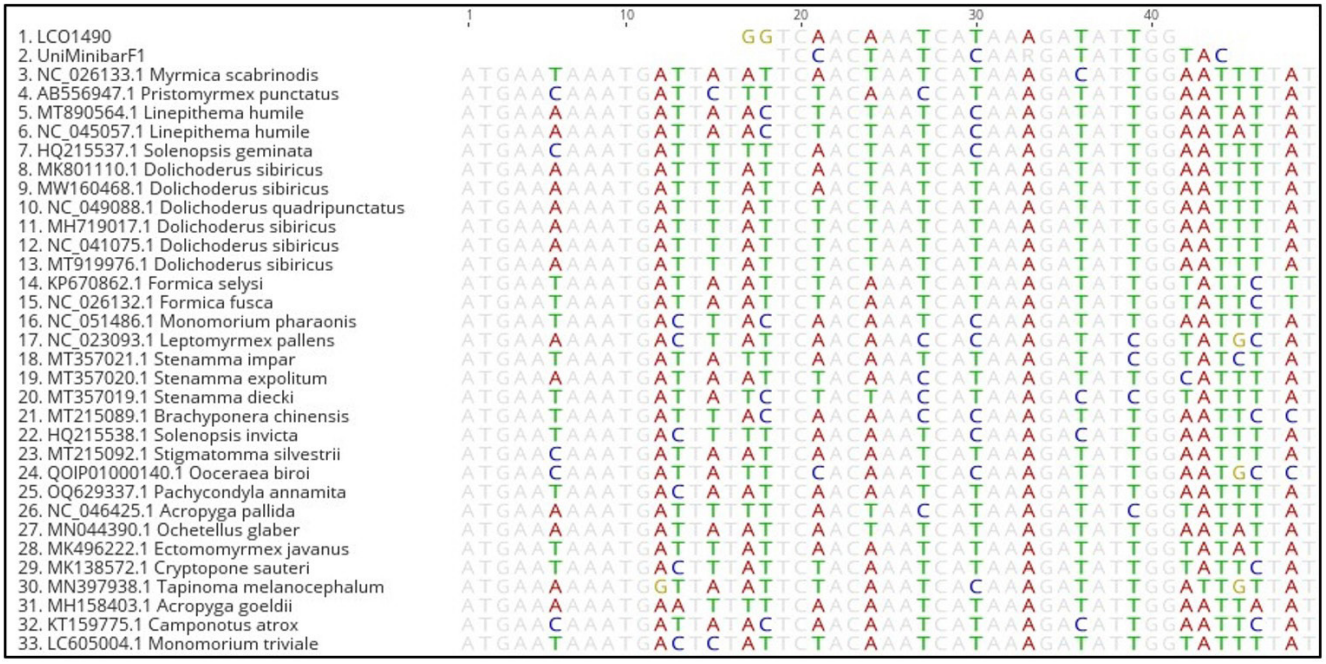

Figure 1. Annealing position of forward primers for DNA barcoding (LCO1490) and mini-barcoding (UniMinibarF1) for the COI gene of several ant species

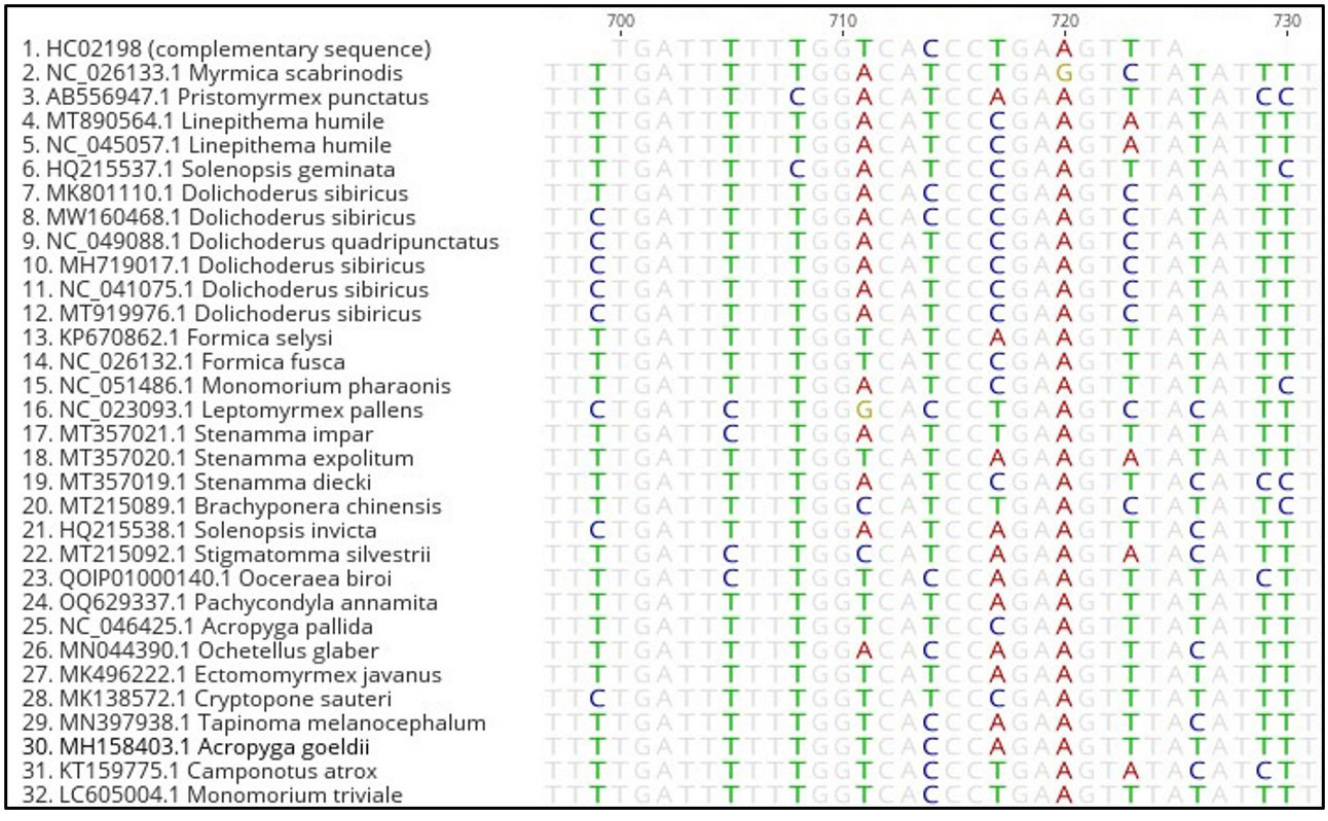

Figure 2. Annealing position of reverse primer for DNA barcoding (HC02198, represented by the complementary sequence) in the COI gene of several ant species

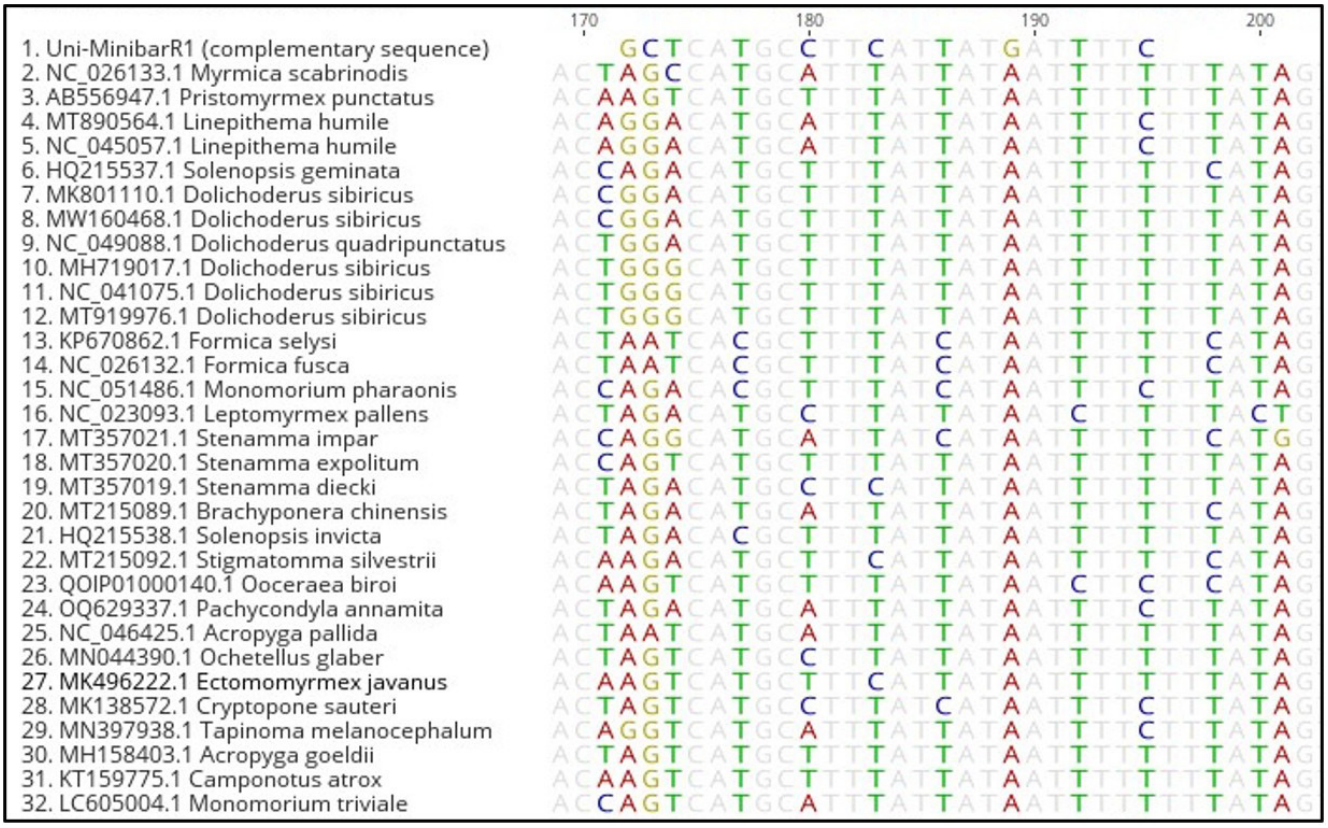

Figure 3. Annealing position of reverse primer for mini-barcoding (Uni-MinibarR1, represented by the complementary sequence) in the COI gene of several ant species

positions 45 and 171, which was used as the mini-barcode fragment. A direct comparison between the 658-base-pair DNA barcode and the 127-base-pair mini-barcode, specifically in ant species, has not been previously reported.

Primer annealing to the target sequence is a critical requirement for successful PCR amplification. For the DNA barcoding forward primer LCO1490, eight nucleotide positions were found to differ from the aligned ant COI sequences. At the third nucleotide from the 3′ end (nucleotide position 39; Figure 1), the primer contains T, which is replaced by C in several ant species, including *Leptomyrmex pallens, Stenamma impar, S. diecki*, and *Acropyga pallida*. Likewise, at the sixth nucleotide from the 3′ end (nucleotide position 36; Figure 1), the primer sequence contains T, which alternates with C in species such as *Myrmica scabrinodis, S. diecki, Solenopsis invicta*, and *Camponotus atrox*. In addition, two further mismatches were identified at nucleotide positions 27 and 30 (Figure 1), where T in the LCO1490 primer corresponds to C in various ant species. One of these mismatches occurs near the center of the primer, while the other is located closer to the 5′ end. At nucleotide position 24 (Figure 1), A in the primer aligns with T in the sequence alignment, and at position 21, A in the primer corresponds to either T or C in the target sequences. Furthermore, the two nucleotides at the 5′ end of the LCO1490 primer also show mismatches when aligned with the ant COI sequences.

The mini-barcoding forward primer UniMinibarF1 exhibited nine nucleotide mismatches with the aligned COI sequences of ant species (Figure 1), including two located at the 3′ end of the primer (nucleotide positions 42 and 44). At nucleotide position 43, the primer sequence contains A, which is conserved across all ant species except *Tapinoma melanocephalum*, in which T is present. At position 44, the primer contains C, whereas the corresponding position in the ant sequences contains T. As the terminal nucleotide at the 3′ end does not match the target sequence in any of the ant species examined, this primer may require further optimization for reliable PCR amplification in Formicidae.

The DNA barcoding reverse primer HCO2198 exhibited seven nucleotide differences when

compared with the aligned COI sequences of the ant species (Figure 2). The five nucleotides at the 3′ end of the primer (positions 700 to 704) matched the consensus sequence in the ant alignment. Notably, G at position 701, which corresponds to C in the actual primer due to strand complementarity, contributes to the formation of a GC clamp (Lowe *et al.* 1990), potentially enhancing the specificity of primer binding. At nucleotide positions 705 and 708, the alignment showed variation between T and C, whereas the primer contains a thymine, corresponding to A in the reverse complement sequence. A similar variation was observed at position 714, where the primer has C, corresponding to G in the reverse complement. Nucleotide position 711 displayed the greatest variability, with all four nucleotides (T, A, G, and C) observed among the ant sequences.

For the reverse mini barcoding primer UniMinibarR1, sequence variation was observed at 10 nucleotide positions across the aligned ant COI sequences (Figure 3). Notably, considerable variation was detected at the 3′ end of the primer binding site, particularly within the last three nucleotides, which are highly variable and not reflected in the primer sequence. The G at the terminal 3′ position of the primer was present in only 9 of the 31 specimens (29 percent), suggesting a substantial risk of PCR failure, as correct pairing at the 3′ terminus is essential for successful DNA extension. Furthermore, the second nucleotide (C) from the 3′ end in the primer did not match any of the nucleotides present at that position in the ant sequences, which were either C or A. These mismatches at critical positions may reduce primer efficiency, and the design of an alternative reverse primer that avoids these variable sites may be necessary to improve amplification success in ant specimens.

3.2. Comparison of Species Identification by DNA barcoding vs. Mini-barcoding

Species identification using DNA barcoding has commonly been conducted on fresh tissue samples (von Cräutlein *et al.* 2011; Jiao *et al.* 2020; Nehal *et al.* 2021). In contrast, the recovery of DNA from degraded specimens, whether due to suboptimal storage conditions or long-term preservation, has emphasized the utility of mini barcoding (Meusnier *et al.* 2008; Appleyard *et al.* 2022; Jaume-Schinkel *et al.* 2024; Li *et al.* 2024). Mini-barcoding relies on shorter DNA fragments, making it more suitable for compromised genetic material. However, the reliability of mini-barcoding for accurate species identification still requires critical evaluation. To date, no direct comparison between standard DNA barcoding and mini-barcoding has been conducted specifically for ant species using COI gene sequences. Therefore, the present comparison provides important baseline data that may inform future applications in molecular taxonomy and biodiversity studies involving the Formicidae family.

Multiple sequence alignment of 31 ant specimens revealed that the COI gene segment corresponding to the Folmer region (658 base pairs) is generally effective for distinguishing ant species (Table 2). Sequence similarity among the same species (intraspecific) in DNA barcoding was between 92.9 to 100% (with 86.9% as average), and in mini-barcoding was between 91.3 to 100% (with 95% as average). The interspecific sequence similarity in DNA barcoding ranged from 70.1 to 98.8% (with an average of 72.0%), and in mini-barcoding, it ranged from 64.6 to 99.2% (with an average of 89%). A close similarity is shown by *Dolichoderus quadripunctatus* (NC_049088.1) with all of the *Dolichoderus sibiricus* specimens. A complete sequence match (100% similarity) was observed only between *D. sibiricus* (MH719017.1) and *D. sibiricus* (NC_041075.1), as both records represent the same species. Among other *D. sibiricus* specimens, sequence similarity ranged from 92.7 to 99.7%. In the case of mini-barcoding, three specimens identified as *D. sibiricus* (MH719017.1, NC_041075.1, dan (MT919976.1)) and two specimens identified as *L. humile* (MT890564.1 and NC_045057.1) shared identical sequences.

Sequence comparison within the Folmer region revealed the lowest similarity value, 71.4%, between *Formica fusca* (NC_026132.1) and *Leptomyrmex pallens* (NC_023093.1). In the mini-barcoding dataset, these two specimens exhibited a slightly lower similarity of 64.6%, although this was not the lowest observed across all pairwise comparisons. The lowest similarity based on mini-barcoding was found between *L. pallens* (NC_023093.1) and *Pachycondyla annamita* (OQ629337.1). When *L. pallens* (NC_023093.1) was compared with the remaining 30 specimens, 26 exhibited mini-barcode similarity values below 70%. In the case of full-length DNA barcoding, *L. pallens* (NC_023093.1) showed similarity values below 80% in all comparisons, with the exception of *Monomorium triviale* (LC605004.1).

Table 2. Pairwise sequence similarity among ant species based on DNA barcoding (658 base pairs) and mini barcoding (127 base pairs)

#	Specimen & Accession	Similarity (%)																															
		1	2	3	4	5	6	7	8	9	10	11	12	13	14	15	16	17	18	19	20	21	22	23	24	25	26	27	28	29	30	31	
1	*Myrmica scabrinodis* (NC_026133.1)		77.2	85.0	85.0	89.0	83.5	82.7	83.5	83.5	83.5	83.5	89	87.4	78.7	65.4	80.3	86.6	86.6	76.4	88.2	81.1	79.5	84.3	84.3	84.3	85.0	78.0	81.9	84.3	76.4	83.5	
2	*Pristomyrmex punctatus* (AB556947.1)	79.2		75.6	75.6	81.1	76.4	75.6	76.4	76.4	76.4	76.4	76.4	75.6	74.8	68.5	74.0	78.0	77.2	72.4	78.7	75.6	66.1	77.2	74.0	75.6	74.0	70.9	75.6	78.0	70.1	76.4	
3	*Linepithema humile* (MT890564.1)	80.4	78.3		100	86.6	83.5	82.7	81.9	81.9	81.9	81.9	77.2	76.4	77.2	67.7	79.5	80.3	78.7	79.5	84.3	78.0	78.0	79.5	77.2	89.0	86.6	76.4	81.1	78.7	75.6	78.0	
4	*Linepithema humile* (NC_045057.1)	80.2	78.1	99.8		86.6	83.5	82.7	81.9	81.9	81.9	81.9	77.2	76.4	77.2	67.7	79.5	80.3	78.7	79.5	84.3	78.0	78.0	79.5	77.2	89.0	86.6	76.4	81.1	78.7	75.6	78.0	
5	*Solenopsis geminata* (HQ215537.1)	79.3	80.2	79.0	78.9		85.0	84.3	83.5	83.5	83.5	83.5	80.3	79.5	80.3	64.6	80.3	85.0	82.7	74.8	92.9	77.2	75.6	79.5	81.9	81.9	80.3	74.8	78.7	80.3	76.4	81.9	
6	*Dolichoderus sibiricus* (MK801110.1)	78.9	79.2	81.3	81.2	79.6		99.2	92.1	92.1	92.1	92.1	78.7	78.0	82.7	65.4	79.5	81.1	79.5	75.6	81.1	85.0	73.2	80.3	76.4	81.1	80.3	76.4	81.1	83.5	71.7	79.5	
7	*Dolichoderus sibiricus* (MW160468.1)	78.9	79.0	81.2	81.0	79.6	98.8		91.3	91.3	91.3	91.3	78.0	77.2	81.9	64.6	78.7	80.3	80.3	74.8	80.3	84.3	72.4	79.5	75.6	80.3	79.5	75.6	80.3	82.7	72.4	78.7	
8	*Dolichoderus quadripunctatus* (NC_049088.1)	79.8	78.9	81.3	81.2	80.1	92.7	92.2		99.2	99.2	99.2	81.1	81.9	80.3	67.7	78.0	79.5	79.5	78.7	81.1	81.1	74.0	81.9	77.2	81.1	80.3	80.3	78.7	83.5	70.1	78.7	
9	*Dolichoderus sibiricus* (MH719017.1)	79.5	79.2	80.9	80.7	79.3	92.9	93.0	97.0		100	100	81.1	81.9	80.3	66.9	78.0	79.5	80.3	78.7	81.1	81.1	74.8	82.7	77.2	81.1	80.3	81.1	78.7	83.5	70.1	79.5	
10	*Dolichoderus sibiricus* (NC_041075.1)	79.5	79.2	80.9	80.7	79.3	92.9	93.0	97.0	100		100	81.1	81.9	80.3	66.9	78.0	79.5	80.3	78.7	81.1	81.1	74.8	82.7	77.2	81.1	80.3	81.1	78.7	83.5	70.1	79.5	
11	*Dolichoderus sibiricus* (MT919976.1)	79.5	79.2	80.9	80.7	79.6	93.2	93.0	97.3	99.7	99.7		81.1	81.9	80.3	66.9	78.0	79.5	80.3	78.7	81.1	81.1	74.8	82.7	77.2	81.1	80.3	81.1	78.7	83.5	70.1	79.5	
12	*Formica selysi* (KP670862.1)	83.0	80.4	79.6	79.5	80.5	78.6	78.7	78.1	79.3	79.3	79.3		97.6	75.6	65.4	74.0	80.3	79.5	79.5	80.3	81.1	74.0	81.9	81.9	78.7	81.1	78.7	76.4	83.5	74.0	79.5	
13	*Formica fusca* (NC_026132.1)	83.1	79.8	79.9	79.8	79.9	78.3	78.4	78.1	79.3	79.3	79.3	98.8		76.4	65.4	73.2	80.3	79.5	78.0	79.5	81.1	73.2	81.1	81.9	78.0	81.1	79.5	75.6	82.7	73.2	78.0	
14	*Monomorium pharaonis* (NC_051486.1)	78.1	77.5	76.7	76.6	79.9	79.2	79.0	78.6	79.6	79.6	79.3	80.4	80.1		66.9	76.4	78.0	78.0	74.8	78.0	81.9	70.9	74.0	73.2	78.7	75.6	76.4	81.1	78.7	74.8	81.9	
15	*Leptomyrmex pallens* (NC_023093.1)	71.4	72.3	73.3	73.1	74.2	72.5	72.5	74.2	72.2	72.2	72.2	72	71.4	73.3		65.4	66.1	66.1	68.5	66.9	69.3	66.9	64.6	65.4	71.7	70.1	66.9	71.7	67.7	73.2	64.6	
16	*Stenamma impar* (MT357021.1)	76.7	77.5	75.8	75.7	79.0	75.5	76.0	74.6	74.8	74.8	74.6	75.4	74.8	76.9	72.3		78.7	84.3	76.4	81.9	77.2	75.6	73.2	71.7	76.4	75.6	73.2	75.6	74.8	72.4	78.0	
17	*Stenamma expolitum* (MT357020.1)	80.7	80.5	80.1	79.9	81.6	78.9	78.7	78.0	77.8	77.8	77.8	82.5	82.7	79.8	72.9	77.4		81.9	76.4	84.3	82.7	74.0	81.9	82.7	76.4	81.9	78.7	77.2	79.5	74.8	85.8	
18	*Stenamma diecki* (MT357019.1)	79.2	78.4	76.9	76.7	79.8	79.3	79.3	78.7	78.3	78.3	78.4	78.9	78.6	78.9	72.6	82.5	79.9		79.5	80.3	80.3	78.7	79.5	74.8	77.2	78.7	78.0	81.1	81.9	78.0	82.7	
19	*Brachyponera chinensis* (MT215089.1)	78.1	76.9	79.3	79.2	77.5	77.5	77.4	78.6	79.2	79.2	79.2	79.9	79.8	78.7	73.6	74.8	78.9	76.9		75.6	78.0	79.5	81.9	70.9	77.2	79.5	78.0	73.2	80.3	73.2	78.7	
20	*Solenopsis invicta* (HQ215538.1)	80.7	80.4	77.7	77.8	85.9	78.4	78.1	79.0	79.0	79.0	79.3	79.5	79.8	79.6	74.0	79.8	79.6	78.4	78.4		77.2	71.7	77.2	81.1	81.1	79.5	77.2	78.0	80.3	74.8	80.3	
21	*Stigmatomma silvestrii* (MT215092.1)	80.9	78.1	79.2	79.0	79.5	79.9	80.1	79.0	78.7	78.7	78.7	83.0	83.1	79.5	74.3	77.4	81.6	79.6	80.7	77.7		74.8	79.5	78.0	78.7	84.3	78.0	81.1	84.3	74.8	80.3	
22	*Ooceraea biroi* (QOIP01000140.1)	77.8	77.2	77.2	77.1	76.6	77.2	76.7	76.4	76.6	76.6	76.9	78.6	78.3	76.3	70.1	76.3	76.7	77.8	75.4	76.0	78.4		74.8	71.7	76.4	78.0	72.4	72.4	75.6	73.2	75.6	
23	*Pachycondyla annamita* (OQ629337.1)	80.1	80.9	79.3	79.5	76.9	79.6	79.9	80.1	80.5	80.5	80.5	82.5	82.2	78.4	70.5	75.1	81.2	78.6	83.4	78.1	83.3	76.6		77.2	79.5	83.5	78.0	73.2	78.0	69.3	79.5	
24	*Acropyga pallida* (NC_046425.1)	81.6	79.5	79.5	79.3	78.4	78.3	78.3	78.3	78.6	78.6	78.6	81.8	82.2	77.8	72.2	75.2	80.7	76.4	76.4	77.8	79.5	76.3	79.0		79.5	75.6	72.4	75.6	78.0	68.5	77.2	
25	*Ochetellus glaber* (MN044390.1)	80.2	81.8	85.7	85.6	79.6	82.1	82.4	81.3	81.8	81.8	82.1	81.9	81.6	78.7	73.6	76.6	78.7	78.4	79.0	78.7	80.4	78.0	82.5	82.4		85.0	77.2	81.1	81.1	71.7	74.8	
26	*Ectomomyrmex javanus* (MK496222.1)	80.4	79.5	81.5	81.3	78.4	79.0	78.7	78.0	77.5	77.5	77.7	82.1	82.1	77.1	73.4	76.0	81.3	77.5	80.5	77.8	84.2	77.4	83.1	78.9	82.2		84.3	79.5	81.9	76.4	77.2	
27	*Cryptopone sauteri* (MK138572.1)	78.6	77.5	77.1	76.9	77.4	75.8	76.6	78.3	78.4	78.4	78.4	78.6	79.0	78.0	71.9	75.1	78.6	76.1	81.2	78.9	79.5	74.8	81.8	76.7	78.7	81.9		75.6	78.0	73.2	78.0	
28	*Tapinoma melanocephalum* (MN397938.1)	79.5	77.7	83.1	83.0	78.1	82.1	81.6	81.6	81.9	81.9	81.9	79.9	79.8	78.0	74.6	76.4	78.3	78.3	78.1	78.3	79.3	75.1	78.9	78.0	83.9	78.1	77.7		78.0	76.4	81.1	
29	*Acropyga goeldii* (MH158403.1)	81.5	80.4	77.8	77.7	78.4	79.2	79.5	77.7	78.6	78.6	78.4	84.0	84.3	77.7	71.6	76.4	79.6	79.9	80.9	78.1	83.0	77.1	81.8	81.2	82.5	82.5	79.2	79.2		72.4	78.7	
30	*Camponotus atrox* (KT159775.1)	78.4	76.9	77.1	76.9	77.8	75.1	74.9	75.2	74.6	74.6	74.6	78.7	78.4	77.1	76.0	75.5	78.9	76.9	76.3	76.7	78.6	74.8	75.8	77.4	77.2	77.5	75.1	75.4	77.2		76.4	
31	*Monomorium triviale* (LC605004.1)	78.6	79.0	77.5	77.4	81.0	79.3	79.5	77.8	79.6	79.6	79.5	81.9	81.2	84.0	72.5	77.8	80.2	79.9	78.7	79.3	78.6	76.6	79.6	79.8	80.9	79.5	80.2	79.5	80.1	76.0		

DNA BARCODING

MINI-BARCODING

These findings indicate that the COI gene functions as an effective standard marker for species-level differentiation in ants. DNA barcoding and mini-barcoding were able to be performed for species identification through sequence homology. Although both species in the genus *Dolichoderus* require special attention due to their close similarity, mini-barcoding with a shorter sequence was capable of distinguishing them. The size of the sequence does matter, but even the shorter sequence still served its purpose as a tool for species identification for ants.

3.3. Genetic Distance Comparison between DNA Barcoding and Mini-Barcoding in Ant Specimens

Genetic distance of 31 ant specimens revealed that the Folmer region (658 base pairs) represents ant species taxonomically (Table 3). The intra-specific distance in DNA barcoding was between 0 and 0.091 (with 0.049 as average), and in mini-barcoding was between 0 to 0.127 (with 0.068 as average). The inter-specific distance in DNA barcoding was between 0.029 to 0.836 (with 0.512 as average), and in mini-barcoding was between 0.009 to 1.466 (with 0.621 as average). Both *Dolichoderus sibiricus* (MH719017.1) and *D. sibiricus* (NC_041075.1) specimens that are identical, as mentioned before in species identification, showed zero in distance. For mini-barcoding, four specimens shared identical sequences. It was between *D. sibiricus* (MH719017.1, NC_041075.1, and MT919976.1) and between *L. humile* (MT890564.1 and NC_045057.1).

3.4. Barcode Length and Its Impact on Species Discrimination in Ants

The comparison between full-length DNA barcoding and mini-barcoding revealed differences in their capacity to resolve taxonomic and phylogenetic relationships among ant species (Table 4). Both approaches successfully amplified and analyzed the COI region, with nucleotide lengths of 658 bp for the full-length barcode and 127 bp for the mini-barcode. The mini-barcode showed slightly higher intra-specific identity (91.3–100%, average 95%) compared to the full-length barcode (92.9–100%, average 86.9%), indicating high sequence similarity within species despite the shorter fragment. Interestingly, inter-specific identity was also higher in the mini-barcode (64.6–99.2%, average 89%) than in the full-length barcode (70.1–98.8%, average 72.0%), suggesting a potential reduction in discriminatory power due to the limited sequence length.

In terms of genetic distance, the full-length barcode had a lower average intraspecific distance (0.049) than the mini-barcode (0.068), indicating better resolution of within-species variation. Similarly, average inter-specific distance was lower in full-length barcodes (0.512) compared to mini-barcodes (0.621), although the maximum divergence observed was higher in the latter (1.466 versus 0.836). These results demonstrate that while mini-barcoding is effective for species identification—particularly in degraded samples—full-length barcoding remains superior for capturing fine-scale genetic divergence both within and between ant species.

3.5. Comparison of Phylogenetic Resolution between DNA Barcoding vs. Mini-barcoding

The mitochondrial COI gene is widely used to infer phylogenetic relationships among species (Achint and Singh 2021; Prakrongrak *et al.* 2023; Abdoli *et al.* 2024; Walia and Dhillon 2024). As illustrated in Figures 4 and 5, both DNA barcoding (658 base pairs) and mini-barcoding (127 base pairs) were able to cluster species from the same genus into distinct clades. For example, *Dolichoderus sibiricus* consistently grouped with *D. quadripunctatus* in both datasets, indicating congruent placement across marker lengths. The same thing also occurs with the genus Formica and the genus *Linepithema*. While the DNA barcoding provided greater internal branch resolution and higher bootstrap support overall, the shorter mini-barcoding fragment also retained sufficient phylogenetic signal to distinguish closely related taxa. These findings suggest that both marker types can contribute to taxonomic resolution, though standard barcoding may offer enhanced reliability in deeper or more complex clades.

Variation in s equence length can substantially influence the phylogenetic placement of certain specimens. A clear example is *Acropyga pallida* (NC_046425.1), which appears distantly related to the genus *Dolichoderus* when analyzed using the full-length Folmer region. In contrast, the mini-barcoding dataset places this species within the *Dolichoderus* clade. This inconsistency highlights the limitations of shorter sequences, which may reduce the accuracy of phylogenetic inference. Overall, the longer Folmer region provides greater reliability for reconstructing phylogenetic trees, offering improved resolution and

Table 3. Pairwise genetic distances among ant species based on DNA barcoding (658 base pairs) and mini-barcoding (127 base pairs)

#	Specimen & Accession	Distance																														
		1	2	3	4	5	6	7	8	9	10	11	12	13	14	15	16	17	18	19	20	21	22	23	24	25	26	27	28	29	30	31
1	*Myrmica scabrinodis* (NC_026133.1)		0.587	0.345	0.345	0.160	0.323	0.332	0.332	0.341	0.341	0.341	0.227	0.257	0.486	1.015	0.470	0.273	0.380	0.664	0.211	0.472	0.771	0.430	0.370	0.404	0.438	0.764	0.408	0.410	0.663	0.392
2	*Pristomyrmex punctatus* (AB556947.1)	0.448		0.753	0.753	0.467	0.731	0.740	0.740	0.749	0.749	0.749	0.803	0.833	0.894	1.423	0.877	0.681	0.788	1.071	0.477	0.880	1.178	0.951	0.757	0.812	0.845	1.171	0.816	0.818	1.071	0.799
3	*Linepithema humile* (MT890564.1)	0.440	0.537		0	0.325	0.349	0.358	0.357	0.367	0.367	0.367	0.561	0.591	0.458	0.987	0.541	0.439	0.452	0.689	0.376	0.497	0.796	0.709	0.536	0.202	0.254	0.580	0.380	0.435	0.635	0.558
4	*Linepithema humile* (NC_045057.1)	0.441	0.538	0.002		0.325	0.349	0.358	0.357	0.367	0.367	0.367	0.561	0.591	0.458	0.987	0.541	0.439	0.452	0.689	0.376	0.497	0.796	0.709	0.536	0.202	0.254	0.580	0.380	0.435	0.635	0.558
5	*Solenopsis geminata* (HQ215537.1)	0.385	0.365	0.475	0.476		0.303	0.312	0.312	0.321	0.321	0.321	0.375	0.405	0.466	0.995	0.450	0.253	0.360	0.644	0.090	0.452	0.751	0.523	0.329	0.384	0.418	0.744	0.388	0.390	0.643	0.372
6	*Dolichoderus sibiricus* (MK801110.1)	0.433	0.531	0.390	0.392	0.468		0.009	0.109	0.118	0.118	0.118	0.539	0.569	0.490	1.018	0.519	0.417	0.430	0.667	0.354	0.403	0.774	0.687	0.513	0.407	0.441	0.767	0.411	0.341	0.666	0.535
7	*Dolichoderus sibiricus* (MW160468.1)	0.440	0.537	0.396	0.398	0.475	0.012		0.118	0.127	0.127	0.127	0.548	0.578	0.499	1.028	0.528	0.426	0.439	0.676	0.363	0.412	0.783	0.696	0.523	0.417	0.450	0.776	0.420	0.350	0.675	0.545
8	*Dolichoderus quadripunctatus* (NC_049088.1)	0.426	0.523	0.383	0.384	0.461	0.087	0.093		0.009	0.009	0.009	0.548	0.578	0.498	1.027	0.528	0.426	0.439	0.675	0.363	0.412	0.783	0.695	0.522	0.416	0.449	0.776	0.420	0.350	0.675	0.544
9	*Dolichoderus sibiricus* (MH719017.1)	0.424	0.522	0.381	0.382	0.459	0.085	0.091	0.032		0	0	0.557	0.587	0.508	1.037	0.537	0.435	0.448	0.685	0.372	0.421	0.792	0.705	0.532	0.426	0.459	0.785	0.429	0.359	0.684	0.554
10	*Dolichoderus sibiricus* (NC_041075.1)	0.424	0.522	0.381	0.382	0.459	0.085	0.091	0.032	0		0	0.557	0.587	0.508	1.037	0.537	0.435	0.448	0.685	0.372	0.421	0.792	0.705	0.532	0.426	0.459	0.785	0.429	0.359	0.684	0.554
11	*Dolichoderus sibiricus* (MT919976.1)	0.421	0.519	0.378	0.379	0.456	0.082	0.088	0.029	0.003	0.003		0.557	0.587	0.508	1.037	0.537	0.435	0.448	0.685	0.372	0.421	0.792	0.705	0.532	0.426	0.459	0.785	0.429	0.359	0.684	0.554
12	*Formica selysi* (KP670862.1)	0.393	0.437	0.482	0.484	0.375	0.476	0.482	0.468	0.467	0.467	0.464		0.030	0.702	1.231	0.686	0.489	0.596	0.879	0.426	0.688	0.986	0.645	0.585	0.620	0.653	0.979	0.624	0.626	0.879	0.608
13	*Formica fusca* (NC_026132.1)	0.397	0.442	0.486	0.488	0.379	0.480	0.487	0.473	0.471	0.471	0.468	0.013		0.732	1.261	0.716	0.519	0.626	0.909	0.456	0.718	1.017	0.675	0.616	0.650	0.683	1.010	0.654	0.656	0.909	0.638
14	*Monomorium pharaonis* (NC_051486.1)	0.459	0.439	0.549	0.550	0.336	0.542	0.549	0.535	0.533	0.533	0.530	0.449	0.453		0.974	0.682	0.580	0.593	0.830	0.517	0.638	0.937	0.850	0.677	0.517	0.550	0.877	0.367	0.576	0.622	0.699
15	*Leptomyrmex pallens* (NC_023093.1)	0.665	0.710	0.755	0.756	0.648	0.748	0.755	0.741	0.739	0.739	0.736	0.640	0.644	0.722		1.211	1.109	1.122	1.359	1.046	1.167	1.466	1.379	1.205	1.046	1.079	1.405	0.895	1.105	0.559	1.227
16	*Stenamma impar* (MT357021.1)	0.508	0.454	0.597	0.599	0.426	0.591	0.597	0.584	0.582	0.582	0.579	0.498	0.502	0.500	0.770		0.563	0.262	0.859	0.501	0.668	0.967	0.833	0.660	0.600	0.634	0.960	0.604	0.606	0.859	0.682
17	*Stenamma expolitum* (MT357020.1)	0.466	0.413	0.556	0.557	0.384	0.549	0.556	0.542	0.540	0.540	0.537	0.456	0.460	0.458	0.729	0.432		0.474	0.757	0.304	0.565	0.864	0.636	0.463	0.498	0.531	0.857	0.501	0.504	0.757	0.258
18	*Stenamma diecki* (MT357019.1)	0.485	0.432	0.575	0.576	0.403	0.569	0.575	0.561	0.559	0.559	0.556	0.475	0.480	0.477	0.748	0.255	0.409		0.770	0.411	0.578	0.877	0.744	0.571	0.511	0.544	0.870	0.515	0.517	0.770	0.593
19	*Brachyponera chinensis* (MT215089.1)	0.583	0.627	0.672	0.673	0.565	0.666	0.672	0.658	0.657	0.657	0.654	0.463	0.467	0.639	0.830	0.687	0.646	0.665		0.694	0.815	0.505	1.027	0.854	0.748	0.781	1.107	0.751	0.753	1.006	0.876
20	*Solenopsis invicta* (HQ215538.1)	0.429	0.409	0.518	0.519	0.191	0.512	0.518	0.504	0.503	0.503	0.500	0.418	0.423	0.379	0.691	0.469	0.427	0.446	0.608		0.503	0.802	0.574	0.380	0.435	0.469	0.795	0.439	0.441	0.694	0.423
21	*Stigmatomma silvestrii* (MT215092.1)	0.432	0.477	0.521	0.523	0.414	0.515	0.521	0.508	0.506	0.506	0.503	0.312	0.316	0.488	0.679	0.537	0.495	0.514	0.401	0.458		0.922	0.835	0.662	0.556	0.589	0.915	0.559	0.397	0.815	0.684
22	*Ooceraea biroi* (QOIP01000140.1)	0.573	0.520	0.663	0.664	0.491	0.656	0.663	0.649	0.647	0.647	0.644	0.563	0.568	0.565	0.836	0.471	0.497	0.448	0.753	0.534	0.602		1.134	0.961	0.855	0.888	1.214	0.858	0.861	1.114	0.983
23	*Pachycondyla annamita* (OQ629337.1)	0.526	0.570	0.615	0.617	0.508	0.609	0.615	0.602	0.600	0.600	0.597	0.406	0.410	0.582	0.773	0.631	0.589	0.608	0.308	0.551	0.345	0.696		0.733	0.768	0.801	1.127	0.771	0.773	1.026	0.755
24	*Acropyga pallida* (NC_046425.1)	0.371	0.468	0.439	0.440	0.406	0.432	0.439	0.425	0.423	0.423	0.420	0.413	0.418	0.480	0.686	0.528	0.487	0.506	0.603	0.449	0.452	0.594	0.546		0.594	0.628	0.954	0.598	0.600	0.853	0.582
25	*Ochetellus glaber* (MN044390.1)	0.421	0.519	0.230	0.231	0.456	0.372	0.378	0.364	0.362	0.362	0.359	0.464	0.468	0.530	0.736	0.579	0.537	0.556	0.653	0.499	0.503	0.644	0.597	0.420		0.313	0.639	0.439	0.494	0.694	0.616
26	*Ectomomyrmex javanus* (MK496222.1)	0.510	0.555	0.600	0.601	0.493	0.593	0.600	0.586	0.584	0.584	0.581	0.390	0.395	0.567	0.757	0.615	0.574	0.593	0.380	0.536	0.329	0.681	0.323	0.531	0.581		0.395	0.472	0.527	0.727	0.650
27	*Cryptopone sauteri* (MK138572.1)	0.573	0.618	0.663	0.664	0.556	0.657	0.663	0.649	0.647	0.647	0.644	0.454	0.458	0.630	0.821	0.678	0.637	0.656	0.443	0.599	0.392	0.744	0.386	0.594	0.644	0.334		0.798	0.854	1.053	0.976
28	*Tapinoma melanocephalum* (MN397938.1)	0.418	0.515	0.290	0.292	0.453	0.368	0.375	0.361	0.359	0.359	0.356	0.460	0.465	0.527	0.733	0.575	0.534	0.553	0.650	0.496	0.499	0.641	0.593	0.417	0.272	0.578	0.641		0.498	0.543	0.620
29	*Acropyga goeldii* (MH158403.1)	0.438	0.483	0.528	0.529	0.421	0.521	0.528	0.514	0.512	0.512	0.509	0.319	0.323	0.495	0.686	0.543	0.502	0.521	0.467	0.464	0.317	0.609	0.411	0.459	0.509	0.395	0.458	0.506		0.753	0.622
30	*Camponotus atrox* (KT159775.1)	0.461	0.506	0.550	0.552	0.443	0.544	0.551	0.537	0.535	0.535	0.532	0.436	0.440	0.517	0.450	0.566	0.524	0.544	0.625	0.487	0.475	0.632	0.569	0.482	0.532	0.553	0.616	0.529	0.481		0.875
31	*Monomorium triviale* (LC605004.1)	0.465	0.445	0.554	0.555	0.341	0.548	0.554	0.540	0.539	0.539	0.535	0.454	0.459	0.257	0.727	0.505	0.463	0.482	0.644	0.385	0.494	0.570	0.587	0.485	0.535	0.572	0.635	0.532	0.500	0.523	

DNA BARCODING

MINI-BARCODING

Table 4. Comparison of DNA barcoding and mini-barcoding for species identification and phylogeny in ants

Category	DNA Barcoding	Mini-barcoding
PCR amplicon size	709 bp	177 bp
Nucleotide length for analysis	658 bp	127 bp
Intra-specific barcode identity	92.9-100% (avg. 86.9%)	91.3-100% (avg.95%)
Inter-specific barcode identity	70.1-98.8% (avg.72.0%)	64.6-99.2% (avg.89%)
Intra-specific genetic distance	0-0.091 (avg. 0.049)	0-0.127 (avg. 0.068)
Inter-specific genetic distance	0.029-0.836 (avg. 0.512)	0.009-1.466 (avg. 0.621)

a more consistent representation of evolutionary relationships among ant species.

4. Discussion

The selection of appropriate primers is pivotal for the success of PCR-based DNA barcoding, particularly in taxa with high genetic variability such as ants. The widely used "Folmer" primers, LCO1490 and HCO2198, were originally designed based on sequences from marine invertebrates (Folmer *et al.* 1994). While these primers have demonstrated broad utility across

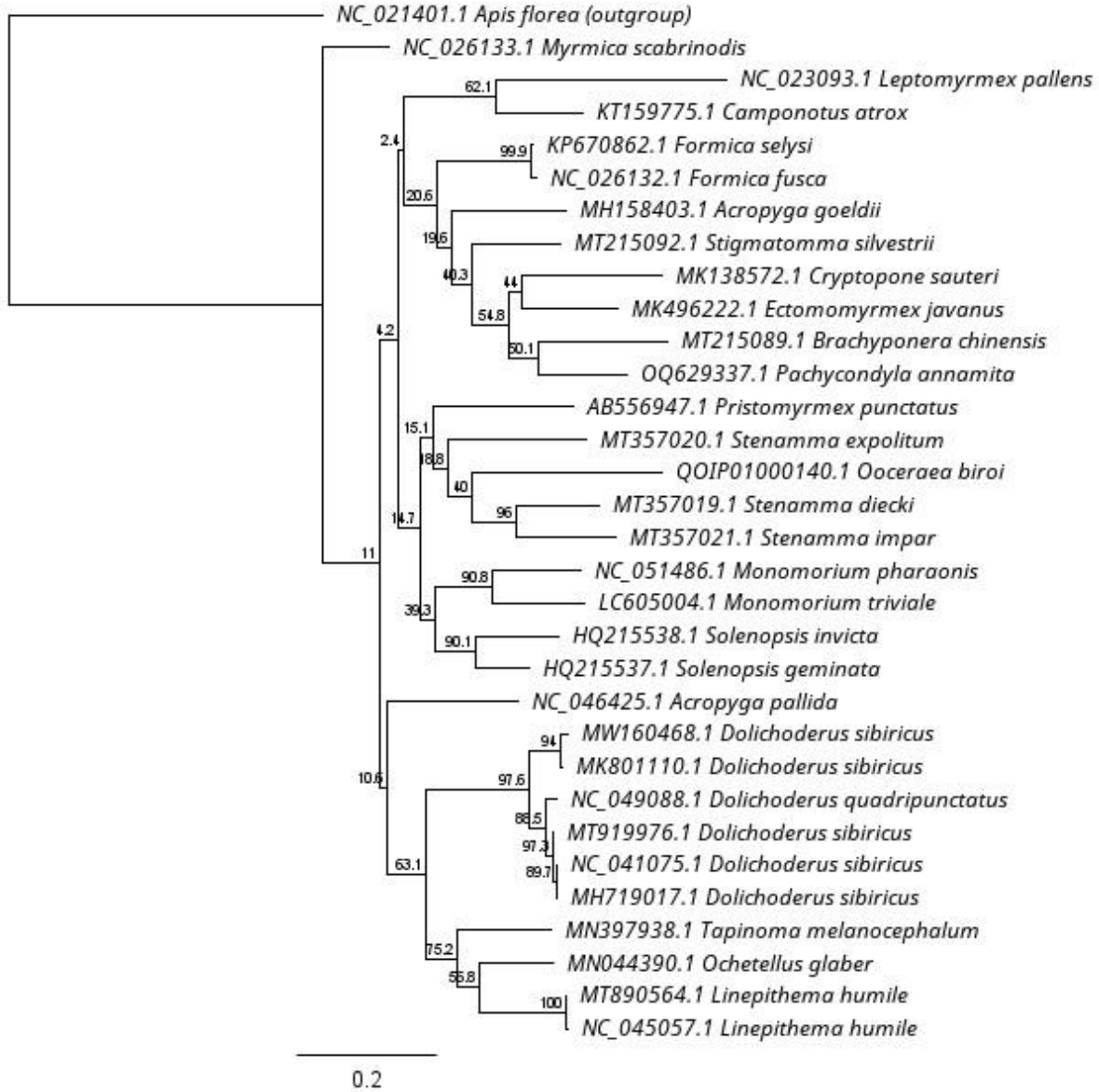

Figure 4. Maximum likelihood phylogenetic tree of ant species based on 658 base pairs of the COI gene (DNA barcoding region), constructed using the Tamura-Nei model with 1,000 bootstrap replicates

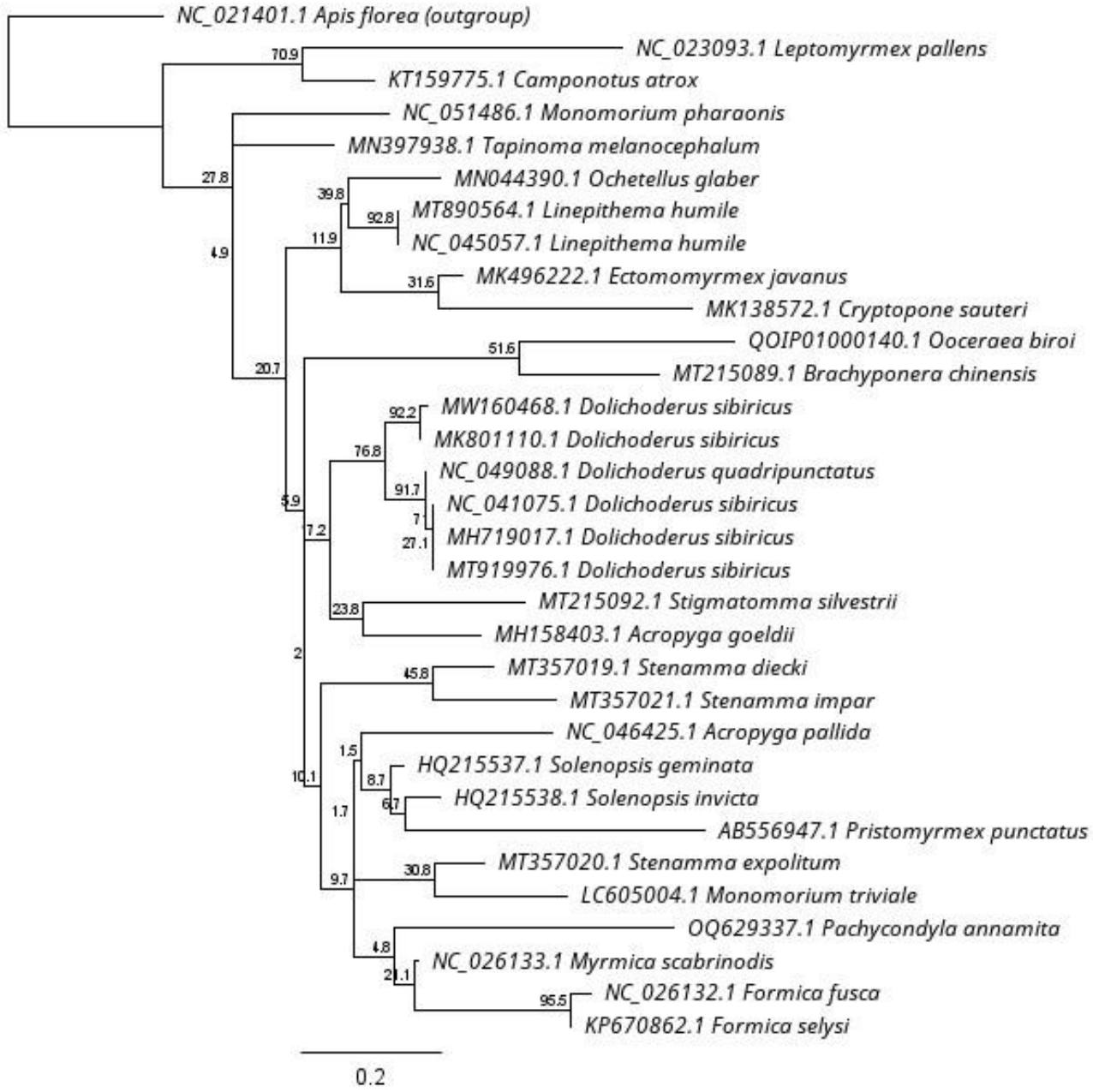

Figure 5. Maximum likelihood phylogenetic tree of ant species based on 127 base pairs of the COI gene (mini-barcoding region), constructed using the Tamura-Nei model with 1,000 bootstrap replicates

various metazoan taxa, subsequent studies have identified limitations in their universality, especially concerning insects. For instance, Clarke *et al.* (2014) and Elbrecht and Leese (2017) reported mismatches at primer binding sites in insect taxa, leading to reduced amplification efficiency.

In line with prior research demonstrating that primer-template mismatches can limit PCR efficiency (Stadhouders *et al.* 2010; Elbrecht & Leese 2017), our results underscore the importance of refining standard primers for ant-specific applications. Targeted adjustments to the LCO1490 sequence, particularly at sites influencing the GC clamp, could improve annealing efficiency and broaden taxonomic coverage. Similar modifications have been successfully applied in other insect groups (Pentinsaari *et al.* 2016). The adjustment is likely to enhance amplification reliability in Formicidae, where even minor mismatches can affect PCR success.

Thermodynamic evaluation using OligoAnalyzer (Owczarzy *et al.* 2008) indicates that the modified LCO1490 primer has a melting temperature (Tm)

between 56.5°C and 59.8°C and a predicted hairpin formation temperature below 17.1°C, suggesting acceptable primer performance for downstream applications. The reverse primer HCO2198, when aligned with the ant COI sequences, showed seven nucleotide variations. However, none of these mismatches occur within the critical five nucleotides at the 3′ end, which are essential for effective annealing. This observation is consistent with findings by Stadhouders *et al.* (2010), who emphasized the importance of the 3′ terminal region in primer binding efficiency. Therefore, modification of HCO2198 is not currently deemed necessary for the ant COI amplification.

Regarding mini-barcoding primers, UniMinibarF1, designed for broad taxonomic coverage including degraded samples (Meusnier *et al.* 2008), presents critical mismatches at the 3′ end in ants. Such mismatches can significantly impair PCR success, as even single mismatches at the 3′ terminal base can reduce amplification efficiency (Kwok *et al.* 1990). Our findings suggest that UniMinibarF1 is suboptimal for ants and may be replaced with the modified LCO1490, given their overlapping binding sites.

The reverse mini-barcode primer UniMinibarR1 also showed mismatches at its internal 3′ region, notably positions 172–174, which are highly variable across Formicidae. Designing a new primer starting from position 175, with adjustments based on sequence consensus, yielded a proposed sequence with improved binding potential and acceptable thermodynamic properties, aligning with primer design recommendations by Ye *et al.* (2012).

Primer properties and barcode length both influence the taxonomic and phylogenetic resolution of DNA barcoding. In this study, both the 658 bp full-length barcode and the 127 bp mini-barcode successfully differentiated all ant species. However, longer sequences captured greater intraspecific variation, as observed in *D. sibiricus* and *L. humile*, where full-length COI data revealed subtle divergence not detected by the shorter fragment. This finding is consistent with Meier *et al.* (2006), who noted that while mini-barcodes are generally adequate for species identification, they are less informative for population-level or phylogenetic analyses.

The observed intraspecific variation in some specimens may also be influenced by colony structure, as ants exhibit both monogyny (single queen) and polygyny (multiple queens), which can affect mitochondrial DNA variation due to maternal inheritance. In polygynous species such as *L. humile* and *Dolichoderus* spp., the presence of multiple reproductive queens can lead to higher mitochondrial diversity within a species, potentially contributing to the subtle divergence observed.

Phylogenetic analyses further highlighted differences in resolution, as shown in the genetic distances. Although both barcode lengths clustered congeners such as *D. sibiricus* and *D. quadripunctatus*, discrepancies emerged in deeper relationships. In our analysis, *Acropyga pallida* exhibited differing phylogenetic placements depending on the sequence length used, highlighting the limitations of short mitochondrial fragments in resolving deeper evolutionary relationships. This observation aligns with previous studies indicating that shorter mitochondrial sequences often lack sufficient phylogenetic information, leading to reduced topological stability and potential misinterpretations in phylogenetic analyses. For instance, Chan *et al.* (2022) have demonstrated that short 16S rRNA fragments can produce inaccurate phylogenetic reconstructions with lower and more variable branch support, erratic genetic distances, and overestimated species delimitation partitions due to insufficient phylogenetic information content.

Studies have shown that complete mitochondrial genomes provide more robust phylogenetic signals than single mitochondrial genes, offering higher resolution and more precise date estimates (Zhang *et al.* 2021; Finnegan *et al.* 2025). This suggests that while mini-barcoding remains a useful tool for species-level identification, full-length DNA barcoding or complete mitochondrial genomes are preferred for more accurate phylogenetic inference.

Therefore, in order to achieve reliable phylogenetic placements and understand evolutionary relationships accurately, especially in taxa like ants where subtle genetic differences are significant, utilizing longer mitochondrial sequences is recommended. Consequently, careful primer optimization and appropriate barcode length selection are essential for enhancing COI-based species identification and phylogenetic analysis. This study supports the refinement of molecular tools for Formicidae and contributes to broader applications in biodiversity assessment and bioinformatics.

In conclusion, DNA barcoding has become a standard approach for species identification across

various taxa, including ants, utilizing universal primers for amplifying the COI gene. In this study, DNA barcoding primer HC02198 is considered reliable for PCR amplification, while LCO1490 showed mismatches within the sequence alignment with one critical variation in the GC-clamp region. The universal mini-barcoding primers encountered significant issues, leading to potential failure in PCR amplification. It is recommended to use LCO1490 as a forward primer for mini-barcoding, while designing a new reverse primer by shifting the annealing site three nucleotides downstream to enhance the success of mini-barcoding for ants. As a tool for species identification, DNA barcoding and mini-barcoding are reliable for this purpose. The same sequences that were employed for species identification comparison demonstrated the ability to be employed in phylogenetic analysis. A longer sequence for species identification and phylogenetic analysis determined better accuracy.

Acknowledgements

The authors sincerely thank the Directorate of Research, Technology, and Community Service, Ministry of Education, Culture, Research, and Technology of the Republic of Indonesia, for their valuable support and assistance. This research was funded through the Doctoral Dissertation Research Scheme under primary contract number 084/E5/PG.02.00.PL/2024 and derivative contract number 1902/UN12.13/LT/2024.

References

Abdelhady, A.A., Seuss, B., Jain, S., Fathy, D., Sami, M., Ali, A., Elsheikh, A., Ahmed, M.S., Elewa, A.M.T., Hussain, A. M., 2024. Molecular technology in paleontology and paleobiology: Applications and limitations. *Quaternary International*. 685, 24-38. https://doi.org/10.1016/j.quaint.2024.01.006

Abdoli, P., Talebi, A. A, Kavallieratos, N. G., Khosravi, R., Bidari, F., 2024. Contribution to the phylogeny of Microgastrinae (Hymenoptera: Braconidae) based on mitochondrial COI and nuclear 28S rDNA genes, with comments on the identity of *Pholetesor circumscriptus* (Nees, 1834). *Journal of Insect Biodiversity and Systematics*. 10, 965-981. https://doi.org/10.61186/jibs.10.4.965

Achint, R., Singh, D., 2021. Application of COI gene for identification of some economically and forensically important muscid flies of India (Diptera: Muscidae). *International Journal of Tropical Insect Science*. 41, 3023-3029. https://doi.org/10.1007/s42690-021-00494-8

Antil, S., Abraham, J. S, Sripoorna, S., Maurya, S., Dagar, J., Makhija, S., Bhagat, P., Gupta, R., Sood, U., Lal, R., Toteja, R., 2023. DNA barcoding, an effective tool for species identification: a review. *Molecular Biology Reports*. 50, 761-775. https://doi.org/10.1007/s11033-022-08015-7

Appleyard, S.A., Maher, S., Miskiewicz, A.G., Lara-Lopez, A., Matis, P., Fielder, D.S., Suthers, I.M., 2022. Genetic and morphological identification of formalin fixed, preserved larval fishes; can we have the best of both worlds? *Journal of Experimental Marine Biology and Ecology*. 553, 151763. https://doi.org/10.1016/j.jembe.2022.151763

Babbucci, M., Basso, A., Scupola, A., Patarnello, T., Negrisolo, E., 2014. Is it an ant or a butterfly? Convergent evolution in the mitochondrial gene order of Hymenoptera and Lepidoptera. *Genome Biology and Evolution*. 6, 3326-3343. https://doi.org/10.1093/gbe/evu265

Berman, M., Austin, C. M., Miller, A.D., 2014. Characterisation of the complete mitochondrial genome and 13 microsatellite loci through next-generation sequencing for the New Caledonian spider-ant *Leptomyrmex pallens*. *Molecular Biology Reports*. 41, 1179-1187. https://doi.org/10.1007/s11033-013-2657-5

von Cräutlein, M., Korpelainen, H., Pietiläinen, M., Rikkinen, J., 2011. DNA barcoding: a tool for improved taxon identification and detection of species diversity. *Biodiversity and Conservation*. 20, 373-389. https://doi.org/10.1007/s10531-010-9964-0

Chan, K.O., Hertwig, S.T., Neokleous, D.N., Flury, J.M., Brown, R.M., 2022. Widely used, short 16S rRNA mitochondrial gene fragments yield poor and erratic results in phylogenetic estimation and species delimitation of amphibians. *BMC Ecology and Evolution.* 22, 37. https:// doi.org/10.1186/s12862-022-01994-y

Clarke, L.J., Soubrier, J., Weyrich, L.S., Cooper, A., 2014. Environmental metabarcodes for insects: *in silico* PCR reveals potential for taxonomic bias. *Molecular Ecology Resources*. 14, 1160-1170. https://doi.org/10.1111/1755-0998.12265

Cuautle, M., Castillo-Guevara, C., Juárez-Juárez, B., Pérez-Toledo, G., 2020. Ants (Hymenoptera: Formicidae) in a temperate ecosystem from La Malinche National Park, Mexico. *Florida Entomologist*. 103, 321-328. https://doi.org/10.1653/024.103.0303

Du, Y., Song, X., Yu, H., Lu, Z., 2019. Complete mitochondrial genome sequence of *Tapinoma melanocephalum* (Hymenoptera: Formicidae). *Mitochondrial DNA Part B Resources*. 4, 3448-3449. https://doi.org/10.1080/23802359.2019.1674205

Duan, X., Qian, Z., 2020. *Acropyga goeldii* voucher ACR103 mitochondrion, complete genome. National Center for Biotechnology Information. Available at: www.ncbi.nlm.nih.gov/nuccore/MH158403.1. [Date accessed: 8 April 2025]

Duan, X., Qian, Z., 2023. *Acropyga pallida* voucher ACR27 mitochondrion, complete genome. National Center for Biotechnology Information. Available at: www.ncbi.nlm.nih.gov/nuccore/NC_046425.1. [Date accessed: 7 April 2025]

Duan, X.Y., Peng, X.Y., Qian, Z.Q., 2016. The complete mitochondrial genomes of two globally invasive ants, the Argentine ant *Linepithema humile* and the little fire ant *Wasmannia auropunctata. Conservation Genetics Resources*. 8, 275-277. https://doi.org/10.1007/s12686-016-0555-6

Edgar, R.C., 2004. MUSCLE: multiple sequence alignment with high accuracy and high throughput. *Nucleic Acids Research*. 32, 1792-1797. https://doi.org/10.1093/nar/gkh340

Elbrecht, V., Leese, F., 2017. Validation and development of COI metabarcoding primers for freshwater macroinvertebrate bioassessment. *Frontiers in Environmental Science*. 5, 1-11. https://doi.org/10.3389/fenvs.2017.00011

Ficetola, G.F., Coissac, E., Zundel, S., Riaz, T., Shehzad, W., Bessière, J., Taberlet, P., Pompanon, F. 2010. An *in silico* approach for the evaluation of DNA barcodes. *BMC Genomics*. 11, 434. https://doi.org/10.1186/1471-2164-11-434

Finnegan, N., Lima, M.G.M., Lynch, J.W. 2025. Mitochondrial DNA for phylogeny building: assessing individual and grouped mtGenes as proxies for the mtGenome in Platyrrhines. *American Journal of Primatology*. 87, e70017. https://doi.org/10.1002/ajp.70017

Folmer, O., Black, M., Hoeh, W., Lutz, R., Vrijenhoek, R., 1994. DNA primers for amplification of mitochondrial cytochrome c oxidase subunit I from diverse metazoan invertebrates. *Molecular Marine Biology and Biotechnology*. 3, 294-299.

Fotso Kuate, A., Hanna, R., Nanga, S.N., Tindo, M., Doumtsop Fotio, A.R.P., Nagel, P., 2022. Species richness, density, activity, and composition of ground-dwelling ants in the humid forest zone of Southern Cameroon: role of vegetation cover and abiotic factors. *Environmental Entomology*. 51, 1150-1157. https://doi.org/10.1093/ee/nvac092

Francis, F., Dumas, M.D., Wisser, R.J., 2017. ThermoAlign: a genome-aware primer design tool for tiled amplicon resequencing. *Scientific Reports*. 7, 44437. https://doi.org/10.1038/srep44437

Gonçalves, L.T., Françoso, E., Deprá, M., 2022. Shorter, better, faster, stronger? comparing the identification performance of full-length and mini-DNA barcodes for apid bees (Hymenoptera: Apidae). *Apidologie*. 53, 55. https://doi.org/10.1007/s13592-022-00958-x

Gostel, M.R., Kress, W.J., 2022. The expanding role of DNA barcodes: indispensable tools for ecology, evolution, and conservation. *Diversity*. 14, 213. https://doi.org/10.3390/d14030213

Gotzek, D., Clarke, J., Shoemaker, D., 2010. Mitochondrial genome evolution in fire ants (Hymenoptera: Formicidae). *BMC Evolutionary Biology*. 10, 300. https://doi.org/10.1186/1471-2148-10-300

Guindon, S., Dufayard, J.F., Lefort, V., Anisimova, M., Hordijk, W., Gascuel, O., 2010. New algorithms and methods to estimate Maximum-Likelihood phylogenies: assessing the performance of PhyML 3.0. *Systematic Biology*. 59, 307-321. https://doi.org/10.1093/sysbio/syq010

Hajibabaei, M., Smith, M.A., Janzen, D.H., Rodriguez, J.J., Whitfield, J.B., Hebert, P.D.N., 2006. A minimalist barcode can identify a specimen whose DNA is degraded. *Molecular Ecology Notes*. 6, 959-964. https://doi.org/10.1111/j.1471-8286.2006.01470.x

Hasegawa, E., Kobayashi, K., Yagi, N., Tsuji, K., 2011. Complete mitochondrial genomes of normal and cheater morphs in the parthenogenetic ant *Pristomyrmex punctatus* (Hymenoptera: Formicidae). *Myrmecological News*. 15, 85-90.

Hebert, P.D.N., Ratnasingham, S., deWaard, J.R., 2003. Barcoding animal life: cytochrome c oxidase subunit 1 divergences among closely related species. *Proceedings Biological Sciences*. 270,96-99. https://doi.org/10.1098/rsbl.2003.0025

Huang, K., Zhang, J., Li, J., Qiu, H., Wei, L., Yang, Y., Wang, C., 2024. Exploring the impact of primer-template mismatches on PCR performance of DNA polymerases varying in proofreading activity. *Genes*. 15, 215. https://doi.org/10.3390/genes15020215

Idogawa, N., Lee, C.C., Yang, C.C.S., Dobata, S., 2021. The complete mitochondrial genome of a parthenogenetic ant *Monomorium triviale* (Hymenoptera: Formicidae). *Mitochondrial DNA Part B Resources*. 6, 2793-2795. https://doi.org/10.1080/23802359.2021.1970632

Jaume-Schinkel, S., Müller, B., Avila-Calero, S., Kukowka, S., Rduch, V., Mengual, X., 2024. Preserving morphology while extracting DNA: a non-destructive field-to-museum protocol for slide-mounted specimens. *Biodiversity Data Journal*. 12, e119448. https://doi.org/10.3897/BDJ.12.e119448

Jiao, L., Lu, Y., He, T., Guo, J., Yin, Y., 2020. DNA barcoding for wood identification: global review of the last decade and future perspective. *IAWA Journal*. 41, 620-643. https://doi.org/10.1163/22941932-bja10041

Kalendar, R., Shevtsov, A., Otarbay, Z., Ismailova, A. 2024. *In silico* PCR analysis: a comprehensive bioinformatics tool for enhancing nucleic acid amplification assays. *Frontiers in Bioinformatics*. 4, 1464197. https://doi.org/10.3389/fbinf.2024.1464197

Kim, M.J., Hong, E.J., Kim, I., 2016. Complete mitochondrial genome of *Camponotus atrox* (Hymenoptera: Formicidae): A new tRNA arrangement in Hymenoptera. *Genome*. 59, 59-74.https://doi.org/10.1139/gen-2015-0080

Kolondam, B.J., Tallei, T.E., Koneri, R., Abas, A.H., Mamahit, J.M.E., 2023. A review on mitochondrial genome of ants (Hymenoptera: Formicidae). *Heca Journal of Applied Sciences*. 1, 4853. https:// doi.org/10.60084/hjas.v1i2.74

Kwok, S., Kellogg, D.E., McKinney, N., Spasic, D., Goda, L., Levenson, C., Sninsky, J.J., 1990. Effects of primer-template mismatches on the polymerase chain reaction: human immunodeficiency virus type 1 model studies. *Nucleic Acids Research*. 18, 999-1005. https://doi.org/10.1093/nar/18.4.999

Li, K., Brownley, A., Stockwell, T.B., Beeson, K., McIntosh, T.C., Busam, D., Ferriera, S., Murphy, S., Levy, S., 2008. Novel computational methods for increasing PCR primer design effectiveness in directed sequencing. *BMC Bioinformatics*. 9, 191. https://doi.org/10.1186/1471-2105-9-191

Li, J., Ulloa, G.M., Mayor, P., Santolalla-Robles, M.L., Greenwood, A.D., 2024. Nucleic acid degradation after long-term dried blood spot storage. *Molecular Ecology Resources*. 24, e13979. https://doi.org/10.1111/1755-0998.13979

Lin, X., Song, N., 2023. The first complete mitochondrial genome of the genus *Pachycondyla* (Formicidae, Ponerinae) and insights into the phylogeny of ants. *Genes*. 14, 1528. https://doi.org/10.3390/genes14081528

Liu, X., Du, W., Wang, C., Wu, Y., Chen, W., Zheng, Y., Wang, M., Liu, H., Yang, Q., Qian, S., Chen, L., Liu, C., 2023. A multilocus DNA mini-barcode assay to identify twenty vertebrate wildlife species. *iScience*. 26, 108275. https://doi.org/10.1016/j.isci.2023.108275

Lombogia, C.A., Posangi, J., Pollo, H.N., Tulung, M., Tallei, T.E., 2020. Assessment of genetic variation in *Apis nigrocincta* (Hymenoptera: Apidae) in Sulawesi revealed by partial mitochondrial cytochrome oxidase I gene sequences. *Scientifica*. 2020, 1609473. https://doi.org/10.1155/2020/1609473

Lowe, T., Sharefkin, J., Yang, S.Q., Dieffenbach, C.W., 1990. A computer program for selection of oligonucleotide primers for polymerase chain reactions. *Nucleic Acids Research*. 18, 1757-1761. https://doi.org/10.1093/nar/18.7.1757

Mason, V.C., Li, G., Helgen, K.M., Murphy, W.J., 2011. Efficient cross-species capture hybridization and next-generation sequencing of mitochondrial genomes from noninvasively sampled museum specimens. *Genome Research*. 21, 1695-1704. https://doi.org/10.1101/gr.120196.111

McKenzie, S.K., Kronauer, D.J.C., 2018. The genomic architecture and molecular evolution of ant odorant receptors. *Genome Research*. 28, 1757-1765. https://doi.org/10.1101/gr.237123.118

Meier, R., Shiyang, K., Vaidya, G., Ng, P.K., 2006. DNA barcoding and taxonomy in Diptera: a tale of high intraspecific variability and low identification success. *Systematic Biology*. 55, 715-728. https://doi.org/10.1080/10635150600969864

Menta, C., Remelli, S., 2020. Soil health and arthropods: from complex system to worthwhile investigation. *Insects.* 11, 54.https://doi.org/10.3390/insects11010054

Messer, J., Cover, S.P., LaPolla, J.S., 2016. *Nylanderia deceptrix* sp. n., a new species of obligately socially parasitic formicine ant (Hymenoptera, Formicidae). *ZooKeys.* 552, 49-65. https://doi.org/10.3897/zookeys.552.6475

Meusnier, I., Singer, G.A., Landry, J.F., Hickey, D.A., Hebert, P.D., Hajibabaei M., 2008. A universal DNA mini-barcode for biodiversity analysis. *BMC Genomics*. 9, 214. https://doi.org/10.1186/1471-2164-9-214

Mitchell, K.J., Rawlence, N.J., 2021. Examining natural history through the lens of palaeogenomics. *Trends in Ecology and Evolution*. 36, 258-267. https://doi.org/10.1016/j.tree.2020.10.005

Nachman, M.W., Beckman, E.J., Bowie, R.C., Cicero, C., Conroy, C.J., Dudley, R., Hayes, T.B., Koo, M.S., Lacey, E.A., Martin, C.H., McGuire, J.A., Patton, J.L., Spencer, C.L., Tarvin, R.D., Wake, M.H., Wang, I.J., Achmadi, A., Álvarez-Castañeda, S.T., Andersen, M.J., Arroyave, J., Austin C.C., Barker, F.K., Barrow, L.N., Barrowclough, G.F., Bates, J., Bauer, A.M., Bell, K.C., Bell, R.C., Bronson, A.W., Brown, R.M., Burbrink, F.T., Burns, K.J., Cadena, C.D., Cannatella, D.C., Castoe, T.A., Chakrabarty, P., Colella, J.P., Cook, J.A., Cracraft, J.L., Davis, D.R., Davis-Rabosky, A.R., D'Elía, G., Dumbacher, J.P., Dunnum, J.L., Edwards S.V., Esselstyn, J.A., Faivovich, J., Fjeldså, J., Flores-Villela, O.A., Ford, K., Fuchs, J., Fujita, M.K., Good, J.M., Greenbaum, E., Greene, H.W., Hackett, S., Hamidy, A., Hanken, J., Haryoko, T., Hawkins, M.T., Heaney, L.R., Hillis, D.M., Hollingsworth, B.D., Hornsby, A.D., Hosner, P.A., Irham, M., Jansa, S., Jiménez, R.A., Joseph, L., Kirchman, J.J., LaDuc, T.J., Leaché, A.D., Lessa, E.P., López-Fernández, H., Mason, N.A., McCormack, J.E., McMahan, C.D., Moyle, R.G., Ojeda, R.A., Olson, L.E., Kin Onn, C., Parenti, L.R., Parra-Olea, G., Patterson, B.D., Pauly, G.B., Pavan, S.E., Peterson, A.T., Poe, S., Rabosky, D.L., Raxworthy, C.J., Reddy, S., Rico-Guevara, A., Riyanto, A., Rocha, L.A., Ron, S.R., Rovito, S.M., Rowe, K.C., Rowley, J., Ruane, S., Salazar-Valenzuela, D., Shultz, A.J., Sidlauskas, B., Sikes, D.S., Simmons, N.B., Stiassny, M.L.J., Streicher, J.W., Stuart, B.L., Summers, A.P., Tavera, J., Teta, P., Thompson, C.W., Timm, R.M., Torres-Carvajal, O., Voelker, G, Voss, R.S., Winker, K., Witt, C., Wommack, E.A., Zink, R.M., 2023. Specimen collection is essential for modern science. *PLoS Biology*. 21, e3002318. https://doi.org/10.1371/journal.pbio.3002318

Nehal, N., Choudhary, B., Nagpure, A., Gupta, R.K., 2021. DNA barcoding: a modern age tool for detection of adulteration in food. *Critical Reviews in Biotechnology*. 41, 767-791. https://doi.org/10.1080/07388551.2021.1874279

Niemann, H.J., Bezeng, B.S., Orton, R.D., Kabongo, R.M., Pilusa, M., van der Bank, M., 2022. Using a DNA barcoding approach to facilitate biosecurity: identifying invasive alien macrophytes traded within the South African aquarium and pond plant industry. *South African Journal of Botany*. 144, 364-376. https://doi.org/10.1016/j.sajb.2021.08.041

Nithaniyal, S., Majumder, S., Umapathy, S., Parani, M., 2021. Forensic application of DNA barcoding in the identification of commonly occurring poisonous plants. *Journal of Forensic and Legal Medicine*. 78, 102126. https://doi.org/10.1016/j.jflm.2021.102126

Ogiso-Tanaka, E., Shimada, D., Ogawa, A., Ishiyama, G., Okumura, K., Hosaka, K., Ishii, C., Nam, K.O., Hoshino, M., Nomura, S., Kakizoe, S., Nakamura, Y., Nishiumi, I., Ito, M.A., Kitayama, T., Tanaka, N., Hosoya, T., Jinbo, U., 2025. DNA specimen preservation using DESS and DNA extraction in museum collections. *Biology*. 14, 730. https://doi.org/10.3390/biology14060730

Owczarzy, R., Tataurov, A.V., Wu, Y., Manthey, J. A., McQuisten, K.A., Almabrazi, H.G., Pedersen, K.F., Lin, Y., Garretson, J., McEntaggart, N.O., Sailor, C.A, Dawson, R.B., Peek, A.S., 2008. IDT SciTools: a suite for analysis and design of nucleic acid oligomers. *Nucleic Acids Research*. 36, 163-169. https://doi.org/10.1093/nar/gkn198

Park, J., Kwon, W., Park, J., 2019a. The complete mitochondrial genome of *Siberian odorous* ant, *Dolichoderus sibiricus* Emery, 1889 (Hymenoptera: Formicidae). *Mitochondrial DNA Part B*. 4, 525-526. https://doi.org/10.1080/23802359.2018.1551091

Park, J., Kwon, W., Park, J. 2019b. The complete mitochondrial genome of *Ectomomyrmex javanus* Mayr, 1867 (Hymenoptera: Formicidae). *Mitochondrial DNA Part B*. 4, 1636-1637. https://doi.org/10.1080/23802359.2019.1604095

Park, J., Kwon, W., Park, J., 2019c. The complete mitochondrial genome of *Cryptopone sauteri* Wheeler, W.M., 1906 (Hymenoptera: Formicidae). *Mitochondrial DNA Part B*. 4, 614-615. https://doi.org/10.1080/23802359.2018.1561231

Park, J., Xi, H., Park, J., 2020a. *Dolichoderus quadripunctatus* mitochondrion, complete genome Available at: www.ncbi.nlm.nih.gov/nuccore/NC_049088.1. [Date accessed: 8 April 2025]

Park, J., Xi, H., Park J., 2020b. The complete mitochondrial genome of *Ochetellus glaber* (Mayr, 1862) (Hymenoptera: Formicidae). *Mitochondrial DNA Part B*. 5, 147-149. https://doi.org/10.1080/23802359.2019.1698356

Park, J., Park, C.H., Park, J., 2021a. Complete mitochondrial genome of the H3 haplotype Argentine ant *Linepithema humile* (Mayr, 1868) (Formicidae; Hymenoptera). *Mitochondrial DNA Part B*. 6, 786-788. https://doi.org/10.1080/23802359.2021.1882900

Park, J., Xi, H., Park, J., 2021b. *Brachyponera chinensis* mitochondrion, complete genome. National Center for Biotechnology Information. Available at: www.ncbi.nlm.nih.gov/nuccore/MT215089.1. [Date accessed: 7 April 2025]

Park, J., Xi, H., Park, J., 2021c. *Stigmatomma silvestrii* mitochondrion, complete genome. Available at: www.ncbi.nlm.nih.gov/nuccore/MT215092.1. [Date accessed: 8 April 2025]

Park, J., Xi, H., Park, J., 2023. Monomorium pharaonis mitochondrion, complete genome. National Center for Biotechnology Information. Available at: www.ncbi.nlm.nih.gov/nuccore/NC_051486.1. [Date accessed: 8 April 2025]

Parr, C.L., Bishop, T.R., 2022. The response of ants to climate change. *Global Change Biology*. 28, 3188-3205. https://doi.org/10.1111/gcb.16140

Pentinsaari, M., Salmela, H., Mutanen, M., Toslin, T., 2016. Molecular evolution of a widely-adopted taxonomic marker (COI) across the animal tree of life. *Science Report*. 6, 35275. https://doi.org/10.1038/srep35275

Prakrongrak, N., Boonsoong, B., Monthatong, M., 2023. Genetic diversity and phylogenetic analysis of mayfly Caenis (Insecta: Ephemeroptera) using Cytochrome C Oxidase I (COI) and 12S rRNA genes from Thailand. *Biodiversitas Journal of Biological Diversity*. 24, 1990-1998. https://doi.org/10.13057/biodiv/d240407

Prosser, S.W.J., deWaard, J.R., Miller, S. E., Hebert P.D.N., 2016. DNA barcodes from century-old type specimens using next-generation sequencing. *Molecular Ecology Resources*. 16, 487-497. https://doi.org/10.1111/1755-0998.12474

Qian, Z., Wu, Y., 2022a. *Stenamma impar* voucher SRR1303380 mitochondrion, complete genome. National Center for Biotechnology Information. Available at: www.ncbi.nlm.nih.gov/nuccore/MT357021.1. [Date accessed: 7 April 2025]

Qian, Z., Wu, Y., 2022b. *Stenamma expolitum* mitochondrion, complete genome. National Center for Biotechnology Information. Available at: www.ncbi.nlm.nih.gov/nuccore/MT357020.1. [Date accessed: 7 April 2025]

Qian, Z., Wu, Y., 2022c. *Stenamma diecki* voucher SRR1303368 mitochondrion, complete genome. National Center for Biotechnology Information. Available at: www.ncbi.nlm.nih.gov/nuccore/MT357019.1. [Date accessed: 8 April 2025]

Ratnasingham, S., Hebert, P.D.N., 2007. BOLD: The barcode of life data system (http://www.barcodinglife.org). *Molecular Ecology Notes*. 7, 355-364. https://doi.org/10.1111/j.1471-8286.2007.01678.x

Rocher, L., Blaya, R., Blaise, C., Bischoff, A., Blight, O., 2022. Species and functional responses of ants to inter-row tillage and vegetation in organic *Mediterranean vineyards. Basic and Applied Ecology*. 65, 126-135. https://doi.org/10.1016/j.baae.2022.11.009

Stadhouders. R., Pas, S.D., Anber, J., Voermans, J., Mes, T.H., Schutten, M., 2010. The effect of primer-template mismatches on the detection and quantification of nucleic acids using the 5' nuclease assay. *Journal of Molecular Diagnostics*. 12, 109-117. https://doi.org/10.2353/jmoldx.2010.090035

Tamura, K., Nei, M., 1993. Estimation of the number of nucleotide substitutions in the control region of mitochondrial DNA in humans and chimpanzees. *Molecular Biology and Evolution*. 10, 512-526.

Virgilio, M., Backeljau, T., Nevado, B., de Meyer, M., 2010. Comparative performances of DNA barcoding across insect orders. *BMC Bioinformatics*. 11, 206. https://doi.org/10.1186/1471-2105-11-206

Walia, G.K., Dhillon, G.K., 2024. DNA barcoding and molecular phylogeny of genus *Pseudagrion* (Odonata: Coenagrionidae) based on mitochondrial COI, ND1 and 16S rRNA genes. *International Journal of Tropical Insect Science*. 44, 1567-1590. https://doi.org/10.1007/s42690-024-01256-y

Wang, T., Zhang, Y., Yang, Z., Liu, Z., Du, Y., 2020. DNA barcoding reveals cryptic diversity in the underestimated genus *Triplophysa* (Cypriniformes: Cobitidae, Nemacheilinae) from the northeastern Qinghai-Tibet Plateau. *BMC Evolutionary Biology*. 20, 151. https://doi.org/10.1186/s12862-020-01718-0

Wang, Z., Liu, X., Liang, D., Wang, Q., Zhang, L., Zhang, P., 2023. VertU: universal multilocus primer sets for eDNA metabarcoding of vertebrate diversity, evaluated by both artificial and natural cases. *Frontiers in Ecology and Evolution*. 11, 1164206. https://doi.org/10.3389/fevo.2023.1164206

Wanna, C., Boonman, N., Phakpaknam, S., Pikulthong, V., Jaitrong, W., Soi-Ampornkul, R., 2022. Species diversity of subterranean ants in Rangsit Marsh, Khlong Luang District, Pathum Thani Province, Thailand. *Biodiversitas Journal of Biological Diversity*. 23, 1283-1292. https://doi.org/10.13057/biodiv/d230312

Xing, R.R., Hu, R.R., Han, J.X., Deng, T.T., Chen, Y., 2020. DNA barcoding and mini-barcoding in authenticating processed animal-derived food: a case study involving the Chinese market. *Food Chemistry*. 309, 125653. https://doi.org/10.1016/j.foodchem.2019.125653

Yang, F., Ding, F., Chen, H., He, M., Zhu, S., Ma, X., Jiang, L., Li, H., 2018. DNA barcoding for the identification and authentication of animal species in traditional medicine. *Evidence-based Complementary and Alternative Medicine*. 2018, 5160254. https://doi.org/10.1155/2018/5160254

Yang, S., Li, X., Cai, L.G., Qian, Z.Q., 2016. Characterization of the complete mitochondrial genome of Formica selysi (Insecta: Hymenoptera: Formicidae: Formicinae). *Mitochondrial DNA Part A*. 27, 3378-3380. https://doi.org/10.3109/19401736.2015.1018229

Ye, J., Coulouris, G., Zaretskaya, I., Cutcutache, I., Rozen, S., Madden, T.L., 2012. Primer-BLAST: a tool to design target-specific primers for polymerase chain reaction. *BMC Bioinformatics*. 13, 134. https://doi.org/10.1186/1471-2105-13-134

Zhang, C.J., Cheng, Y.T., Luo, X.S., Chen, Y., He, Y.C., Li, Y.P., Huang, Z.P, Scott, M.B., Xiao, W., 2023. Quantifying ant diversity and community in a subalpine forest mosaic: a comparison of two methods. *Journal of Insect Conservation*. 27, 813-824. https://doi.org/10.1007/s10841-023-00501-y

Zhang, L., Sun, K., Csorba, G., Hughes, A.C., Jin, L., Xiao, Y., Feng, J., 2021. Complete mitochondrial genomes reveal robust phylogenetic signals and evidence of positive selection in horseshoe bats. *BMC Ecology and Evolution*. 21, 199. https://doi.org/10.1186/s12862-021-01926-2

Zina, V., Ordeix, M., Franco, J.C., Ferreira, M.T., Fernandes, M.R., 2021. Ants as bioindicators of riparian ecological health in Catalonian rivers. *Forests*. 12, 625. https://doi.org/10.3390/f12050625